

Automated IVUS contour detection using intensity features and Radial Basis Function approximation

Maria Papadogiorgaki¹, Vasileios Mezaris¹, Yiannis S. Chatzizisis²,
George D. Giannoglou² and Ioannis Kompatsiaris^{1*}

¹Informatics and Telematics Institute, Centre for Research and Technology Hellas
1st Km Thermi-Panorama Rd, 57001 Thermi-Thessaloniki, Greece

²Cardiovascular Eng. and Atherosclerosis Lab., AHEPA University Hospital
Aristotle University Medical School, 54636 Thessaloniki, Greece

Abstract

Intravascular ultrasound (IVUS) constitutes a valuable technique for the diagnosis and management of coronary atherosclerosis. The detection of lumen and media-adventitia borders in IVUS images represents a necessary step in the utilization of the IVUS data for the reliable quantitative assessment of atherosclerotic lesions. In this paper, a fully automated technique for the detection of lumen and media-adventitia boundaries is developed. This comprises two different steps for contour initialization, one for each corresponding contour of interest, and a procedure for the refinement of the detected contours based on Radial Basis Function approximation. The proposed approach is shown to be capable of performing quick and reliable automated segmentation of IVUS images.

1 Introduction

IVUS is a catheter-based technique that renders two-dimensional cross-sectional images of the coronary arteries, and provides information concerning the lumen and wall morphology. Coronary wall consists of three layers, namely the intima, media and adventitia, whereas in an IVUS image three regions are visually distinguished. These are the lumen, the vessel wall, which consists of the intima and the media layers, and the adventitia plus surroundings, as illustrated in Fig. 1. The above regions are separated by two borders: the lumen border, which corresponds to the lumen-wall interface, and the media-adventitia border [1]. The reliable and quick detection of these two borders is the goal of analysis and also the basic step towards the subsequent 3D reconstruction of the arteries, which can provide additional information regarding the burden of atherosclerosis [2].

Traditionally, the segmentation of IVUS images is performed manually, which is a time-consuming procedure affected by high inter- and intra-user variability. To overcome these limitations, several approaches for semi-automated segmentation have been proposed in the literature, using quite a few variations of active contour models [3]. Despite facilitating the

This work was supported by the Greece-Slovenia Joint R&T Programme on “Knowledge-assisted analysis of medical image and video for doctor decision support applications”, GSRT, 2005-2007, the GSRT A8-PPK06 funded project “Development of Techniques for the Semantic Processing of 3D Intravascular Ultrasound”, the Greek State Scholarships Foundation and the Aristotle University Research Committee.

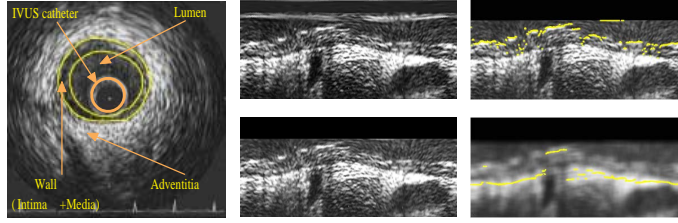


Figure 1. A typical IVUS image with the lumen and media-adventitia borders demarcated, and corresponding polar coordinate images before (right top) and after (right bottom) the removal of catheter-induced artifacts.

analysis of IVUS data as compared to their completely manual processing, the aforementioned methods pose the restriction of needing substantial human intervention during the analysis process. This proves quite restrictive for clinical practice, where fully automated approaches would be most attractive; a limited number of such has been developed so far. In [4], a Hopfield neural network is employed for the modification and minimization of an energy function; however, this method still requires manual estimation of the boundaries in the first frame of the IVUS image sequence. In [5] automatic detection of the endoluminal border is based on an active contour model, whereas in [6] fuzzy clustering is employed; however, both these methods consider the detection of the lumen boundary alone.

This paper presents a novel method for the fully automated segmentation of IVUS images and specifically for the detection of lumen and media-adventitia boundaries. Intensity information is used for the initialization of the contours representing the boundaries of interest, whereas for subsequently smoothing these contours, a technique based on Radial Basis Functions (RBFs) is introduced and compared to a base-line smoothing technique based on low-pass filtering.

The paper is organized as follows: In section 2 image preprocessing is discussed. In sections 3 and 4 the proposed methods for contour initialization and contour refinement are developed. Experimental evaluation and comparisons are reported in section 5 and finally, conclusions are drawn in section 6.

2 IVUS image preprocessing

Preprocessing of the image data for the purpose of contour detection consists of two steps: (a) representation of the images in polar coordinates, and (b) removal of catheter-induced artifacts.

Representation of the images in polar coordinates is important for facilitating the description of local image regions in terms of their radial and tangential characteristics. It also facilitates a number of other detections steps, such as contour initialization and the smoothing of the obtained contour. For this purpose, each of the original IVUS images is transformed to a polar coordinate image where columns and rows correspond to angle and distance from the center of the catheter, respectively, and this image alone, denoted $I(r, \theta)$, is used throughout the analysis process.

The IVUS images include not only tissue and blood regions, but also the outer boundary of the catheter itself. The latter defines a dead zone of radius equal to that of the catheter,

where no useful information is contained. Knowing the diameter D of the catheter, these catheter-induced artifacts are easily removed by setting $I(r, \theta) = 0$ for $r < D/2 + e$, e being a small constant. This preprocessing is illustrated in Fig. 1.

3 Contour initialization

3.1 Lumen contour initialization

Intensity information after the preprocessing stage can be used for detecting the lumen boundary. The latter, when travelling from the center of the catheter towards the image borders on a radius R (i.e. for $\theta = \text{const}$) is typically denoted by an increase of intensity from $I(r, \theta) < e'$, e' being a small constant, to $I(r, \theta) \gg e'$ (e.g. Fig. 1); assuming the presence of no artifacts (noise) in the lumen area, inequality $I(r, \theta) < e'$ should hold for all pixels belonging to the lumen area [7].

Consequently, the lumen contour can be initialized as the set of pixels

$$c_{int,i} = \{\mathbf{p}_{int,i} = [\rho, \theta]\}$$

for which

$$I(\rho, \theta) > T \quad \text{and} \quad I(r, \theta) < T \quad \forall r < \rho$$

This initialization defines a lumen contour function $C_{int,i}(\theta) = \rho$ (Fig. 1). In the above equation, T is a threshold whose value was set experimentally to 128; small deviations from this value were shown to have little effect on the results of initialization.

3.2 Media-adventitia contour initialization

The motivation behind the choice of image data to be used for the initialization of the media-adventitia boundary lies under the proposed approach in the observation that adventitia is represented in the IVUS images by a thick bright ring (a thick bright zone in polar coordinates) that is dominant in the image, as opposed to the media region or any other region of an IVUS image. Consequently, for the localization of the adventitia region, low-pass filtering could be used to suppress undesirable details of the image while preserving well the former [7]. Low-pass filtering, resulting in the generation of a low-pass filtered image I_{LL} , is realized here using the lowpass Haar filter:

$$H(z) = \frac{1}{2}(1 + z^{-1}) \quad (1)$$

Using image I_{LL} , the media-adventitia contour is initialized as the set of pixels

$$c_{ext} = \{\mathbf{p}_{ext} = [\mu, \theta]\}$$

for which

$$I_{LL}(\mu, \theta) = \max_{r > \rho} \{I_{LL}(r, \theta)\},$$

where $[\rho, \theta]$ are the points of the lumen contour, as obtained by the initialization process. This defines a contour function $C_{ext}(\theta) = \mu$ for the media-adventitia contour (Fig. 1).

Selecting, according to the above equations, the pixels to which the intensity of the low-pass filtered image is maximized serves the purpose of identifying the most dominant low-frequency detail in the image, in case low-pass filtering has failed to suppress all other higher-frequency information.

4 RBF-based contour refinement

In contrast to the initial contours generated as described in the previous section, which are not smooth and are characterized by discontinuities (Fig. 1), the true lumen and media-adventitia boundaries are smooth, continuous functions of θ . Consequently, in order to obtain smooth contours that are consistent with the true ones, the application of a filtering or approximation procedure to the initial contour functions $C_{int}(\theta)$, $C_{ext}(\theta)$ is required. In this work, an approach based on RBF approximation is used on the contour functions generated by the initialization process.

Polyharmonic RBFs [8] have been proposed for reconstructing smooth surfaces from point-cloud data and for repairing incomplete meshes through interpolation methods and approximation techniques. Under this approach, the desired smooth surface is defined as the zero set of an RBF s fitted to the given initial surface data. An RBF s is defined as a function of the following form

$$s(x) = p(x) + \sum_{i=1}^N \lambda_i \phi(|x - x_i|), \quad (2)$$

where x is a point in the 2-dimensional or 3-dimensional space, depending on whether the curve to be approximated is a 2D curve or a 3D surface, $p(x)$ is a low degree polynomial, ϕ is a real function called basic function, x_i are the centers of the RBF, λ_i are the RBF coefficients, and $|\cdot|$ denotes here Euclidean distance.

The centers x_i are a subset of points to which a function f is defined, which in turn is defined with respect to the given initial surface data, as discussed in the sequel. Fitting an RBF to the given initial data refers to calculating the RBF coefficients λ_i and the weights of $p(x)$. As basic function ϕ , the biharmonic spline was used in this work:

$$\phi(|x - x_i|) = |x - x_i|^2 \ln(|x - x_i|)$$

The use of an RBF for the approximation of one of the initial contours in a frame, i.e. the generation of a contour c' that is a smooth, reasonable approximation of c , requires the definition for each such contour of a function f , as follows:

$$f(\theta, C(\theta)) = 0$$

where $C(\theta)$ here denotes either $C_{int}(\theta)$ or $C_{ext}(\theta)$, depending on the contour being examined. Function f is used for formulating the approximation problem as one of finding an RBF s for which $s(\cdot) \simeq f(\cdot)$. To avoid the trivial solution of s being zero at every point, f must also be defined for a set of points not belonging to the initial contour (off-surface points), so that

$$f(\theta, r \neq C(\theta)) \neq 0$$

In order to avoid identifying as off-surface points at this stage points which potentially belong to the true contour under examination, the former points are defined in this work as those which satisfy the following equations:

$$r = \max_{\theta} \{C(\theta)\} + 1$$

$$r = \min_{\theta} \{C(\theta)\} - 1$$

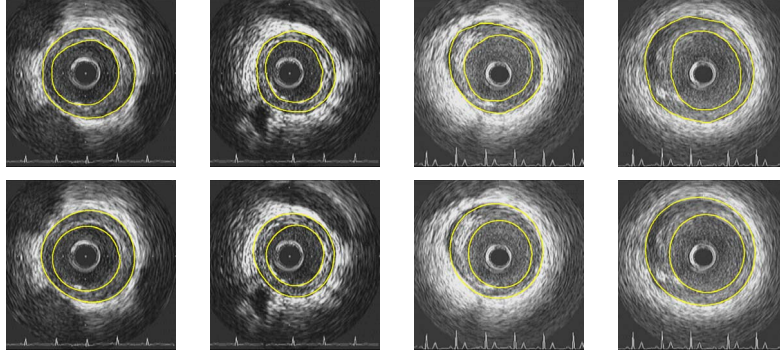


Figure 2. Experimental results for different images of the proposed approach (second row) and comparison with corresponding contours manually generated by experts (first row).

For the above points in the 2D space, function f is defined as the signed Euclidean distance from the initialized contour for $\theta = const$, i.e.

$$f(\theta, r \neq C(\theta)) = r - C(\theta)$$

Following the definition of f , the FastRBF library [9] was used to generate the smooth contour approximation c' by removing duplicate points where f has been defined (i.e. points in the 2D space which are located within a specific minimum distance from other input points; the remaining points serve as the centers of the RBF, x_i , that are defined above), fitting of an RBF to this data and evaluating it to find the points which correspond to zero value; the latter define the contour approximation c' .

5 Experimental results

The methodology developed for the segmentation of IVUS images was applied to 50 images randomly selected from a pool of approximately 300 images belonging to 5 different human coronary arteries. These arterial segments were captured as in [7]. Subsequently, the 50 images comprising our test set were segmented manually by medical experts to generate ground truth results. Indicative results of the proposed method are shown in Fig. 2, where the good agreement of the automatically generated contours with the ground truth results is demonstrated. In table 1, numerical evaluation of the approach proposed in this work versus the manual reference and the method of [7], where low-pass filtering is employed for contour smoothing. Six morphometric parameters are employed, including Cross-sectional areas (Lumen area-LCSA, Vessel area-VCSA, and Wall area-WCSA), maximum diameters (maximum Lumen diameter and maximum Vessel diameter) and maximum Wall thickness. For the calculation of the latter three, the center of gravity of the Lumen area serves as center. The results presented in table 1 using the above parameters reveal the improved performance of the approach using RBFs for the approximation of the initialization results with a smooth continuous function, as compared to our previous approach. The presented results also reveal the sufficient agreement between the results of automated segmentation and the results of manual segmentation.

Table 1. Average error (%) for six IVUS evaluation parameters, calculated from the segmentation results.

| Parameter/ Method | Lumen area (LCSA) | Vessel area (VCSA) | Wall area (WCSA) | max. Lumen diameter | max. Vessel diameter | max. Wall thickness |
|----------------------|----------------------|-----------------------|---------------------|------------------------|-------------------------|------------------------|
| [7] | 14.41% | 8.75% | 17.26% | 11.55% | 6.38% | 25.95% |
| RBFs | 11.49% | 7.82% | 15.23% | 9.38% | 5.85% | 18.81% |

6 Conclusions

In this paper an automated approach for the detection of lumen and media-adventitia boundaries in IVUS images is presented, based on intensity information and the use of RBFs. The proposed approach does not require manual initialization of the contours, which is a common requirement of several other prior approaches to IVUS image segmentation. The experiments conducted with the proposed approach demonstrated its efficiency and the usefulness of the RBF-based approximation technique in generating smooth contours.

References

- [1] G.S. Mintz, S.E. Nissen, W.D. Anderson, S.R. Bailey, R. Erbel, P.J. Fitzgerald, F.J. Pinto, K. Rosenfield, R.J. Siegel, E.M. Tuzcu, and P.G. Yock, "American College of Cardiology Clinical Expert Consensus Document on Standards for Acquisition, Measurement and Reporting of Intravascular Ultrasound Studies (IVUS). A report of the American College of Cardiology Task Force on Clinical Expert Consensus Documents," *Journal of the American College of Cardiology*, vol. 37, pp. 1478–1492, 2001.
- [2] G.D. Giannoglou, Y.S. Chatzizisis, G. Sianos, D. Tsikaderis, A. Matakos, V. Koutkias, P. Diamantopoulos, G.E. Parcharidis, and G.E. Louridas, "Integration of multi-modality imaging for accurate 3D reconstruction of human coronary arteries in vivo," *Nucl Instrum Methods Phys Res A*, 2006.
- [3] J.D. Klingensmith, R. Shekhar, and D.G. Vince, "Evaluation of three-dimensional segmentation algorithms for the identification of luminal and medial-adventitial borders in intravascular ultrasound images," in *IEEE Trans. on Medical Imaging*, 2000, vol. 19, pp. 996–1011.
- [4] M.E. Plissiti, D.I. Fotiadis, L.K. Michalis, and G.E. Bozios, "An Automated Method for Lumen and Media-Adventitia Border Detection in a Sequence of IVUS Frames," *IEEE Trans. on Information Tech. in Biomedicine*, vol. 8, no. 2, June 2004.
- [5] E. Brusseau, C.L. de Korte, F. Mastik, J. Schaar, and A.F.W. van der Steen, "Fully automatic luminal contour segmentation in intracoronary ultrasound imaging - A statistical approach," *IEEE Trans. on Medical Imaging*, vol. 23, pp. 554–566, May 2004.
- [6] E. dos S. Filho, M. Yoshizawa, A. Tanaka, Y. Saijo, and T. Iwamoto, "Detection of Luminal Contour Using Fuzzy Clustering and Mathematical Morphology in Intravascular Ultrasound Images," in *Proceedings of 27th Annual International Conference of the IEEE Engineering in Medicine and Biology (EMBS)*, China, September 2005, pp. 3471–3474.
- [7] G.D. Giannoglou, Y.S. Chatzizisis, V. Koutkias, I. Kompatsiaris, M. Papadogiorgaki, V. Mezaris, E. Parissi, P. Diamantopoulos, M. G. Strintzis, N. Maglaveras, G.E. Parcharidis, and G.E. Louridas, "A Novel Active Contour Model for Fully Automated Segmentation of Intravascular Ultrasound Images: In-Vivo Validation in Human Coronary Arteries," *Computers in Biology and Medicine*, accepted for publication, 2007.
- [8] J.C. Carr, R.K. Beatson, J.B. Cherrie, T.J. Mitchell, W.R. Fright, B.C. McCallum, and T.R. Evans, "Reconstruction and representation of 3D objects with radial basis functions," in *Proceedings of 28th Annual Conference on Computer Graphics and Interactive Techniques*, August 2001, pp. 67–76.
- [9] *FarField Technology*, <http://www.farfieldtechnology.com>.